CORE
Metadata, citation and similar papers at core.ac.uk
Provided by Elsevier - Publisher Connector

Cell, Vol. 84, 941–951, March 22, 1996, Copyright ©1996 by Cell Press

Budding of Rabies Virus Particles in the Absence of the Spike Glycoprotein

Teshome Mebatsion,* Matthias König,† and Karl-Klaus Conzelmann*
*Institute of Clinical Virology
Federal Research Centre for Virus Diseases of Animals
Paul-Ehrlich-Strasse 28
D-72076 Tübingen
Federal Republic of Germany
†Institute of Virology
University of Giessen
D-35392 Giessen
Federal Republic of Germany

Summary

Budding of enveloped viruses from cellular membranes is believed to depend on the presence of transmembrane spike proteins interacting with cytoplasmic virus components. To address the mechanism of rhabdovirus budding, we generated rabies virus mutants deficient for the glycoprotein G or the G cytoplasmic tail. We found that spikeless rhabdovirus particles were released from cells infected with the G-deficient mutant, demonstrating that a viral surface protein is not required to drive the budding process. However, particle production is enhanced approximately 6-fold and 30-fold in the presence of tailless G or G, respectively. This reveals that G also possesses an intrinsic and independent exocytosis activity. We propose a model according to which efficient budding of rhabdoviruses is achieved by a concerted action of both core and spike proteins.

Introduction

Enveloped viruses are released from the infected cell by a mechanism similar to exocytotic budding. During this process, viral core complexes are enveloped by host cell membranes that contain the viral spike proteins almost exclusively. Direct interactions between the cytoplasmic regions of transmembrane spike glycoproteins and the viral cores have been seen as being responsible both for the exclusion of host cell proteins and for the induction of the budding process itself (reviewed by Simons and Garoff, 1980). For hepadnaviruses (Bruss and Ganem, 1991) and alphaviruses (Suomalainen et al., 1992), both core and spike were shown to be absolutely required for budding. Moreover, a direct interaction of a tyrosine-based motif in the cytoplasmic tail of semliki forest virus (SFV) E2 spike protein with the SFV core was shown to be essential for budding (Zhao et al., 1994). In contrast, retroviruses seem to employ a different mechanism, since part of the Gag protein is sufficient for particle formation (Delchambre et al., 1989; Gheysen et al., 1989; Rhee et al., 1990). The situation remains unclear for all other viruses. Especially for viruses possessing an internal membrane-associated matrix (M) protein (e.g., most negative-strand RNA viruses), the forces driving the exocytosis process have not yet been elucidated.

Evidence obtained from the rhabdovirus vesicular stomatitis virus (VSV) suggests that effective inclusion of the spike protein G in the envelope of infectious virions depends on interaction with the M protein, the ribonucleoprotein (RNP) complex core, or both (Whitt et al., 1989; Owens and Rose, 1993). However, it is not known whether such an interaction is necessary for the budding process itself. The finding of VSV G protein fragments consisting of the cytoplasmic and transmembrane domains in spikeless VSV particles that are formed after infection of cells with the temperature-sensitive VSV mutant *tsO45* (Metsikkö and Simons, 1986) had suggested that at least the cytoplasmic domain of the G protein is required for budding. An intriguing observation emphasizing the role of G in particle formation was made recently, after expression of the VSV G protein from an SFV replicon RNA. Infectious vesicles containing naked SFV RNA and VSV spikes were generated, which could be propagated in cell culture (Rolls et al., 1994). This indicates that the VSV G protein can initiate vesicle formation autonomously, without the need to interact with any internal protein and also suggests that rhabdoviruses employ a mechanism of budding that is different from those of either alphaviruses or retroviruses. On the other hand, VSV M protein was reported to bind to the plasma membrane (Chong and Rose, 1993, 1994) and to induce exocytotic budding of vesicles (Li et al., 1993; Justice et al., 1995) in the absence of other VSV proteins.

Experimental analysis of protein interactions and mechanisms involved in virus assembly and release of negative-strand RNA viruses has been limited by the lack of systems that would allow direct genetic manipulation of viruses using recombinant DNA technology. We recently described a reverse genetics system that enabled us to generate recombinant rabies virus (RV) from cDNA (Schnell et al., 1994). The neurotropic RV is the prototype of the lyssavirus genus within the rhabdoviridae family. Its genome organization and virion structure are highly similar to those of VSV. The negative-strand RNA together with the nucleocapsid- (N), phospho- (P), and large (L) protein (polymerase) forms a transcriptionally active RNP. In the virion, the helical RNP is enwrapped by a lipid bilayer containing the single transmembrane glycoprotein G and the matrix protein M associated with the inner side of the membrane. By simultaneous T7 RNA polymerase–driven expression of the RNP proteins N, P, and L, cDNA-derived RV RNA can be incorporated into biologically functional RNPs that are able to initiate an infectious cycle. This approach, which recently has also proved successful in the generation of recombinant VSV (Lawson et al., 1995; Whelan et al., 1995), allowed us to generate helper virus–free RV mutants designed to define the functions of the rhabdovirus G in the course of the viral life cycle.

We describe here the rescue of recombinant RV mutants lacking the genetic information for either the cytoplasmic domain of the G protein or the entire G protein,

as well as the analysis of mutants with regard to formation of virions. The results demonstrate that an interaction between the spike and internal virus proteins is not required to drive the rhabdovirus budding process. Moreover, after infection of cells with phenotypically complemented G-deficient viruses, typical rhabdovirion budding occurred in the absence of G protein. Since the presence of G protein either in its complete or its truncated form enhanced virion yield, we conclude that both the M and the G protein possess an individual (and independent) exocytosis activity. We propose a model according to which optimal budding efficiency and virus production is achieved by a concerted action of both proteins. Accordingly, the role of the spike cytoplasmic tail in budding is indirect, namely, to bring together the separate exocytosis activities of each protein to increase the density of exocytotically active proteins.

Results

Recovery of RV G Mutants from cDNA Clones

The mature RV transmembrane glycoprotein G consists of an amino-terminal N-glycosylated ectodomain of 439 amino acids, a transmembrane anchor sequence of 22 amino acids, and a cytoplasmic domain of 44 amino acids (Anilionis et al., 1981). To address the functions of the cytoplasmic tail involved in the viral assembly and budding process, we constructed a cDNA in which the sequence encoding the entire cytoplasmic tail and the two carboxy-terminal residues of the membrane anchor were deleted (Figure 1). As observed after transient expression in the vaccinia virus/T7 RNA polymerase system, the encoded protein was transported to and anchored in the cell surface membrane (data not shown) and thus fulfilled one of the prerequisites for playing a role in the process of virion formation.

As detailed in Experimental Procedures, the G-encoding sequence of a full-length RV cDNA possessing the authentic sequence of the attenuated RV strain SAD B19 strain (pSAD L16, Schnell et al., 1994; Conzelmann et al., 1990) was replaced by the truncated cDNA. To determine whether we could recover recombinant virus, we used the resulting plasmid pSAD ΔCD for transfection of cells infected with vaccinia vTF7-3 providing T7 RNA polymerase (Fuerst et al., 1986). The RV rescue system is based on the finding that, in cells expressing RV N, P, and L proteins, T7 RNA polymerase transcripts corresponding to RV antigenome RNA are assembled into transcriptionally active RNPs that are able to initiate a productive infection. Since correct encapsidation of preformed RNA is a rare event, successful rescue of standard virus is observed in only 1 in 10^7 transfected cells. With regard to the putative failure of the truncated G protein of SAD ΔCD to support efficiently the initial propagation of the rescued virus, we decided to complement the putative defects by additional expression of wild-type G protein during the rescue and isolation experiments. Thus, in addition to the plasmids encoding RV N, P, and L proteins and pSAD ΔCD, cells were transfected with pT7T-G encoding the SAD B19 G protein (Conzelmann and Schnell, 1994). Cells were lysed in the culture medium 2 days after transfection, and clarified extracts were used to inoculate cells expressing G protein from transfected pT7T-G. After incubation for 2 days, the monolayers were analyzed for the presence of infectious virus by direct immunofluorescence using an anti-N conjugate. In 3 out of 20 experiments, fluorescent foci were identified. A parallel series of rescue experiments in cells not expressing G protein did not result in the isolation of the virus. Therefore, it appears that expression of wild-type G protein is required to support the initial propagation of newly generated viruses and to ensure their recovery. Most interestingly, however, passage of cell-free supernatants from the three cultures to fresh cells reveals that the wild-type G protein is not necessary for further propagation of the recovered recombinant viruses. The finding of autonomously replicating virus from pSAD ΔCD already indicated that the cytoplasmic domain of the RV G protein might be dispensable for virus assembly and budding, as well as for infectivity.

The option to complement a virus deletion mutant successfully by providing the deficient protein in *trans* encouraged us to determine whether an RV mutant lacking the entire G gene could be recovered. A 2.1 kb PflMI–NheI fragment starting within the 3′ nontranslated sequence of the M gene and ending within the 3′ nontranslated sequence of the G gene (SAD B19 position 3177–5339) was deleted from the full-length cDNA clone pSAD L16 (Figure 1A). Accordingly, the resulting pSAD ΔG should encode a 9.8 kb virus genome possessing only four cistrons. pSAD ΔG was used in a transfection series of 20 experiments in the presence of wild-type G protein. After the first passage to cells transiently expressing G protein, fluorescing cells were detected in two cultures. In contrast with SAD ΔCD, however, additional expression of G protein was an absolute requirement for successful further passage, demonstrating a G gene deficiency of the isolated viruses. The identity of the recombinant SAD ΔG and SAD ΔCD viruses was further verified by reverse transcription–polymerase chain reaction (RT–PCR) and by sequencing of PCR products (data not shown). For both viruses, the obtained sequences corresponded exactly to the alterations introduced into the respective cDNA clones. In addition, the PCR experiments also confirmed the absence of standard “helper” RV.

Transcription and Protein Expression of Mutant RVs

To confirm that the alterations introduced into the mutant virus genomes resulted in transcription of the predicted RNA species, we analyzed, by Northern blot hybridization, total RNA from cells infected with SAD ΔCD, SAD ΔG, or SAD L16, respectively. The genome of SAD ΔG was demonstrated by using an N-specific probe. Consistent with the deletion of approximately 2.1 kb in pSAD ΔG, it exhibited a decreased size compared with the standard SAD L16 RV genome (Figure 2A). In contrast, no hybridization of SAD ΔG RNAs was observed with a probe spanning the entire coding region of the RV G gene (Figure 2B). Hybridization with the G probe also confirmed the presence of a truncated G mRNA in cells infected with SAD ΔCD. According to the observed

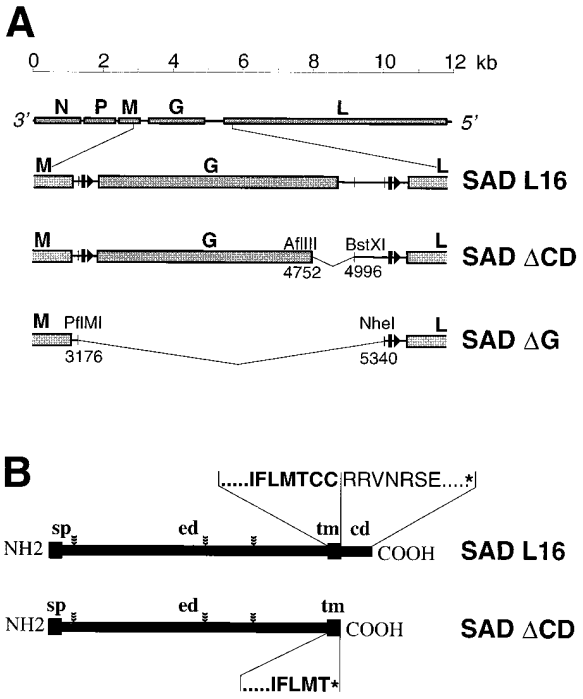

Figure 1. Construction of Recombinant RVs

(A) Organization of recombinant RV genomes. On top, the RV genome with its five open reading frames (boxes) is shown, and in the blowup, the G cistron region is detailed. Closed bars and arrowheads represent transcriptional stop/polyadenylation signals and transcriptional start signals, respectively. Compared with standard RV SAD L16, the genome of SAD ΔCD possesses a deletion spanning the region coding for the cytoplasmic domain of the G protein and part of the nontranslated region (SAD L16 nucleotides 4753–4995). In SAD ΔG, an entire cistron was removed by a deletion starting within the nontranslated region of the M gene and ending close to the transcriptional stop/polyadenylation signal of the G gene (SAD L16 nucleotides 3177–5339).

(B) Comparison of G proteins of SAD L16 and SAD ΔCD. Amino acid residues at the junction of transmembrane (tm) and cytoplasmic domain (cd) are indicated (ed, ectodomain; sp, signal peptide). Branched figures represent potential N-glycosylation sites.

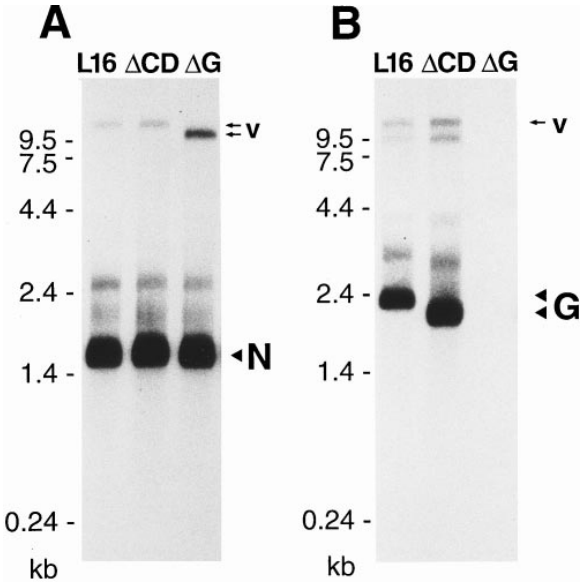

Figure 2. Northern Blot Analysis of Transcripts from Recombinant RVs

Total RNA from cells infected with SAD L16 (L16), SAD ΔCD (ΔCD), and SAD ΔG (ΔG) at a moi of 1 was isolated 2 days postinfection and hybridized with a probe specific for RV N sequences (A) or spanning the entire coding region of the G gene (B). Owing to the deletion of the G gene in the SAD ΔG genome, the viral RNA of SAD ΔG is approximately 2 kb shorter than the standard virus genome (v) and fails to hybridize with the G-specific probe. The decreased size of the SAD ΔCD G mRNA (G) reflects the 0.25 kb deletion of the sequence encoding the cytoplasmic tail of the G protein.

amounts of viral RNAs and mRNAs, neither transcription nor replication of the mutant viruses were markedly affected.

The glycoproteins expressed by SAD ΔCD and SAD L16 were immunoprecipitated from extracts of infected cells with an RV G protein–specific monoclonal antibody (MAb) and analyzed by denaturing SDS–polyacrylamide gel electrophoresis. The G protein encoded by SAD ΔCD virus migrated markedly faster than the G protein of SAD L16. Deglycosylation of precipitated proteins with peptide N-glycosidase F revealed that the observed difference in mobility was due to the truncation of the protein backbone rather than to an altered composition of carbohydrates. Treatment of infected cells with tunicamycin prior to precipitation of proteins further confirmed these results, indicating that the increased electrophoretic mobility of SAD ΔCD G protein reflected the deletion of 46 residues from the carboxyl terminus of RV G protein (Figure 3A).

Since the removal of the cytoplasmic domain of several other viral glycoproteins has been shown to reduce considerably the rate of intracellular transport and the accumulation of proteins at the cell surface (Rose and Bergmann, 1983; Whitt et al., 1989; Jin et al., 1994), we monitored the acquisition of endoglycosidase H–resistant oligosaccharides and cell surface expression. Consistent with previous results on RV G proteins (Whitt et al., 1991; Mebatsion et al., 1995), approximately half of the SAD L16 G protein acquired endoglycosidase H–resistant sugars within 50 min (Figure 3B). A half-time of approximately 60 min was observed for the SAD ΔCD protein lacking the cytoplasmic domain (Figure 3B). As indicated by immunofluorescence microscopy, the slightly reduced transport rate did not reduce accumulation of the truncated protein at the cell surface. To allow a quantitative comparison, we determined the amount of labeled G protein present on the surface of infected cells by immunoprecipitation (Figure 3C). Metabolically labeled infected cells were either directly incubated with the anti-G MAb and lysed after removal of excess antibody (surface) or lysed prior to incubation (total). The specificity of the surface protein precipitation was verified by controls in which unlabeled infected cells were incubated with the MAb and subsequently lysed in the presence of extracts from infected labeled cells (control). According to the radioactivity present in the bands, the amount of G protein present on the surface of cells infected with SAD ΔCD was 86% that of cells infected with SAD L16. In both cases, 18% of total G protein was found at the cell surface.

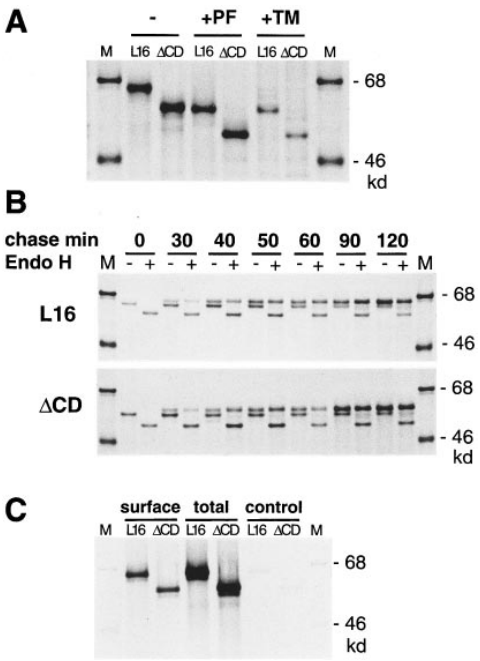

Figure 3. Analysis of G Proteins Encoded by Recombinant RVs

(A) Expression of truncated G protein by SAD ΔCD. [^{35}S]methionine-labeled G proteins from cells infected with SAD L16 (L16) or SAD ΔCD (ΔCD) were precipitated with a MAb and incubated in the presence (plus PF) or absence (minus) of peptide N-glycosidase F. Plus TM, infected cells were labeled in the presence of tunicamycin; M, protein size marker.

(B) Transport kinetics of SAD L16 (L16)– and SAD ΔCD (ΔCD)– encoded G proteins. Proteins pulse labeled for 10 min with [^{35}S]methionine were immunoprecipitated after the indicated chase periods and incubated with (plus) or without (minus) endoglycosidase H for 16 hr. Approximately half of the standard G protein acquired complex oligosaccharides within 50 min, whereas the half-time for the protein lacking the cytoplasmic tail was approximately 60 min.

(C) Cell surface expression of G proteins. Live cells were incubated either directly with anti-G MAb to bind the G protein present at the cell surface (surface) or after lysis of cells (total). To determine the specificity of the assay, we incubated nonlabeled infected cells with the MAb and then lysed them in the presence of extracts from labeled infected cells (control).

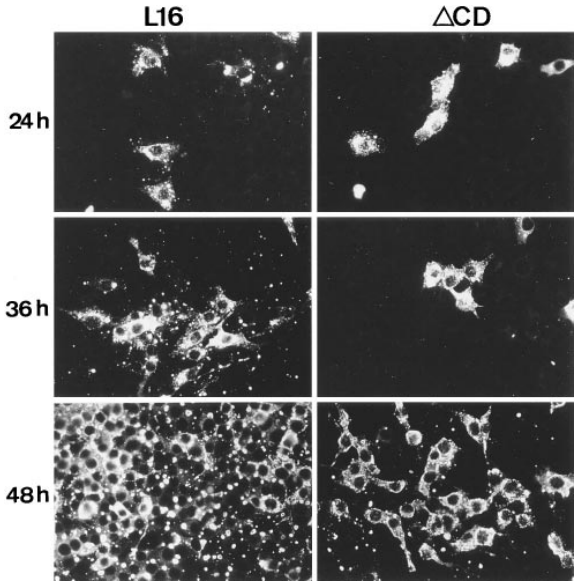

Figure 4. Propagation of Standard SAD L16 RV and SAD ΔCD Encoding a G Protein Lacking the Cytoplasmic Domain in Cell Culture

Following infection of cultures with a moi of 0.01, the spread of infection was monitored at the indicated times by direct immunofluorescence with a conjugate directed against RV N protein. Secondary infection of cells, as indicated by the appearance of small fluorescing granules, is considerably delayed in SAD ΔCD.

Propagation of SAD ΔCD in Cell Culture

The observed autonomous propagation of SAD ΔCD possessing a G protein that lacked the entire cytoplasmic tail proved that this domain is not required for the formation of an infectious agent. However, since the cytoplasmic domain of rhabdovirus G proteins has been shown to be involved in the specificity of incorporation (Owens and Rose, 1993; Whitt et al., 1989), we presumed that such a mutant is hardly viable and may exhibit dramatically altered growth characteristics. Titration of the supernatant obtained from the fourth passage following the rescue experiment revealed a titer of 10^6 focus-forming units per milliliter, which was approximately 100-fold lower than the titer obtained with SAD L16. This stock of SAD ΔCD was further used to analyze virus propagation in more detail. First, cells were infected at a multiplicity of infection (moi) of 0.01 with SAD ΔCD or SAD L16, respectively, and examined by immunofluorescence at 24, 36 and 48 hr postinfection (hpi). In cultures inoculated with SAD L16, primary infection of single cells spread to neighboring cells within 24 hr, as indicated by the appearance of small fluorescent granules (Figure 4). Large foci of 30–50 cells were observed at 36 hpi, and the entire cell monolayer was infected after 48 hr. Conversely, no infection of neighboring cells was observed at 24 hpi in cultures inoculated with SAD ΔCD. In contrast with the large foci observed in SAD L16-infected cultures, only small patches of 5–10 and 20–25 cells were observed at 36 and 48 hpi, respectively (Figure 4). To achieve complete infection of the cell monolayer with SAD ΔCD, an incubation of 72 hr was required (data not shown).

To analyze whether the observed lower titer of the SAD ΔCD stock was due to the reduced ability to spread in cell culture, we performed infections at a moi of 1 and 0.01, and supernatants were titrated at 24, 36, and 48 hpi (Table 1). Since differences between the titers of mutant and wild-type virus were lower when cells were infected at a moi of 1, it appears that the major cause for the divergence is the slower spread of SAD ΔCD. Nevertheless, the observed remaining titer deviation, particularly at early times after infection, confirms the suggestion that the presence of a G protein possessing the cytoplasmic domain is an advantage for efficient budding of virions.

The Cytoplasmic Domain of RV G Protein Ensures Efficient Incorporation of the G Protein into the Envelope of Virions

To address further the reasons for the observed alterations in growth characteristics, we analyzed SAD ΔCD virions for their physical composition, particularly with respect to G content. Supernatants from cells infected at a moi of 1 were collected 2 days postinfection, and virions were purified by velocity centrifugation in 10%–

Table 1. Titers of Recombinant Rabies Viruses

Hours postinfection	Multiplicity of infection	Focus-forming units[a]		SAD ΔCD (Percent)[b]
		SAD L16	SAD ΔCD	
24 hr	0.01	2×10^5	3×10^3	1.5
	1	4×10^6	3.8×10^5	9.5
36 hr	0.01	1×10^7	1.1×10^5	1.1
	1	3×10^7	2.1×10^6	7.0
48 hr	0.01	2×10^8	4×10^5	0.2
	1	8×10^7	6.5×10^6	8.1

[a] Titer of infectious particles (focus-forming units/ml) as determined by endpoint dilution in cell culture.
[b] Ratio of infectious SAD ΔCD virions to SAD L16 virions.

50% sucrose gradients. Viral proteins present in 12 equal fractions from the gradient were analyzed by SDS–polyacrylamide gel electrophoresis and Western blotting. For both SAD ΔCD and SAD L16, the peak of infectivity and the majority of proteins were located in fractions 6 and 7 (Figure 5). However, differences were observed in protein compositions. Whereas the ratios of N, P, and M proteins were similar, SAD ΔCD virions contained a significantly lower amount of G protein relative to the other viral proteins (Figure 5). This indicates that the cytoplasmic domain of the RV G protein is involved in directing the protein into the virion membrane, although considerable amounts of infectious virions are generated in the absence of this function. To facilitate quantitative comparison, we used diluted supernatants from SAD L16–infected cells for gradient centrifugation. As estimated from these experiments (data not shown), the number of virions present in the supernatant of SAD ΔCD–infected cells was 5-fold lower than that found in the supernatant of SAD L16–infected cells.

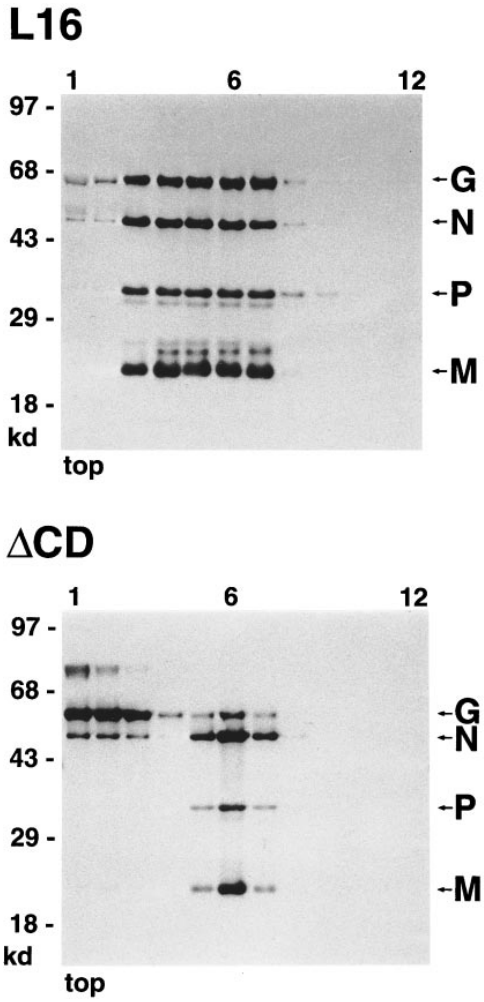

Figure 5. Protein Composition of SAD L16 and SAD ΔCD Virions

Virions from the supernatant of 10^6 infected cells were purified by velocity centrifugation in 10%–50% sucrose gradients. Gradient fractions (1 to 12) were analyzed by Western blotting for the presence of viral proteins. For both preparations, the peak of infectivity was present in fractions 6 and 7. A reduced amount of spike protein (G) relative to the viral N, P, and M proteins is observed in SAD ΔCD virions.

To analyze further the abundance of G protein on the surface of SAD L16 and SAD ΔCD viruses, we examined budding virions by immunoelectron microscopy. Infected cells were fixed with 1% glutaraldehyde at 24 hpi (moi=1), incubated with a MAb directed against RV G protein, and stained with a secondary antibody coupled to colloidal gold. Budding of typical bullet-shaped rhabdovirions was found in cells infected with SAD L16 and SAD ΔCD. More than 90% of budding SAD L16 virions were labeled consistently with several gold particles (Figures 6A and 6B). In contrast, a considerable portion of unlabeled particles was detected in SAD ΔCD–infected cells (Figure 6C). In addition, most labeled SAD ΔCD virions possessed only one or few gold particles, indicating a lower amount of G protein at the viral surface (Figure 6D). Although labeling was not expected to occur at 100% efficiency, the high number of unlabeled SAD ΔCD virions led us to suspect that RV might mature into RV-like particles lacking spike proteins.

Taken together, these findings clearly demonstrate that the cytoplasmic tail of the G protein, and thus, an interaction of the spike protein with internal virus proteins, is not a prerequisite to drive the RV budding process. On the other hand, the presence of the cytoplasmic domain obviously augments the incorporation of spikes into the viral envelope. This results in an approximately 5-fold increase in virion yield, indicating that the G protein contributes to the efficiency of virus budding.

Budding of Noninfectious RV in the Absence of G Protein

As described above, a phenotypically complemented stock of SAD ΔG was grown by five successive passages in cells transiently expressing wild-type G protein from transfected plasmids by the vaccinia virus/T7 RNA–polymerase system. Vaccinia virus was then removed

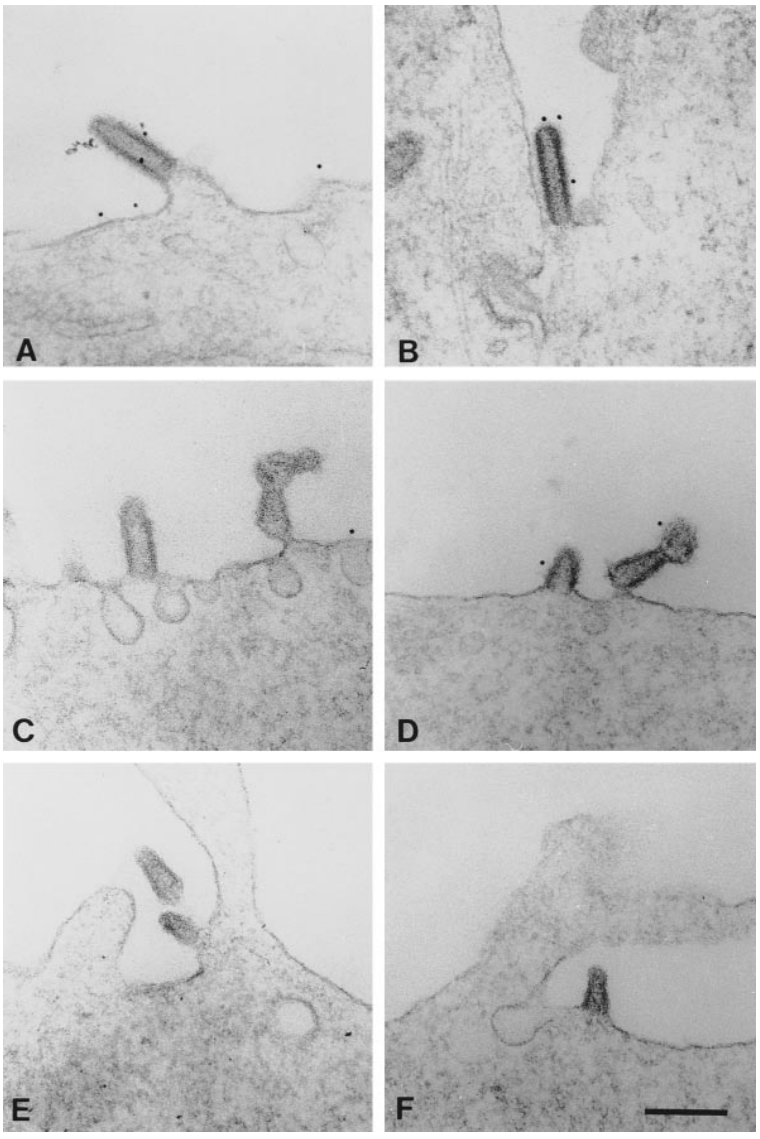

Figure 6. Budding of Recombinant Viruses from the Cell Surface Analyzed by Electron Microscopy

Infected BSR cells were immunostained with a MAb specific for the RV G protein and a gold-conjugated secondary antibody. Labeling with several gold particles was observed for more than 90% of SAD L16 virions (A and B). Both labeled and unlabeled particles budded from cells infected with SAD ΔCD (C and D). (E and F) Budding of noninfectious G-deficient SAD ΔG virions. The bar represents 200 nm.

from the resulting supernatant by filtration. To investigate the growth characteristics of SAD ΔG virus in the absence of exogenous RV G protein expression, we infected cells with high dilutions of the virus stock and examined them by immunofluorescence at various times after infection. N protein–specific fluorescence was detected exclusively in single cells of the confluent monolayers (data not shown). Neither an increase in the number of infected cells nor formation of fluorescent cell foci by cell-to-cell spread was observed during incubation periods of up to 4 days. Thus, infection was absolutely restricted to the primary cells infected by viruses phenotypically complemented with G protein. Assuming one fluorescing cell to result from infection with one infectious unit, the titer of complemented SAD ΔG was 10^6/ml.

Subsequent passaging experiments further verified the absolute requirement of G protein for the infectivity of RV. Cell cultures were inoculated with phenotypically complemented SAD ΔG at a moi of 1, incubated for 1 hr, and washed thoroughly. To neutralize residual input virus, we incubated cells for 30 min with a rabbit serum raised against purified RV G protein. After washing and subsequent incubation for 2 days, supernatants and cell lysates were passaged separately to fresh BSR cell cultures. No fluorescent cells could be detected in these cultures.

To determine whether virions lacking G protein can assemble and bud into the cell culture supernatant, we metabolically labeled infected cultures with [^{35}S]methionine at 16 hpi and chased them for various periods. Cell extracts and pellets from clarified supernatants were analyzed by immunoprecipitation. Most interestingly, viral N, P, and M proteins were detected in the supernatants. Since their ratio was similar to that found for standard virus, the presence of spikeless virions was suggested (Figure 7A). Compared with standard virus infection, however, the amount of released protein was reduced by a factor of 14, 10, and 9 after 3, 6, and 18 hr of chase, respectively, indicating a low budding rate. At corresponding times, release of SAD ΔCD particles

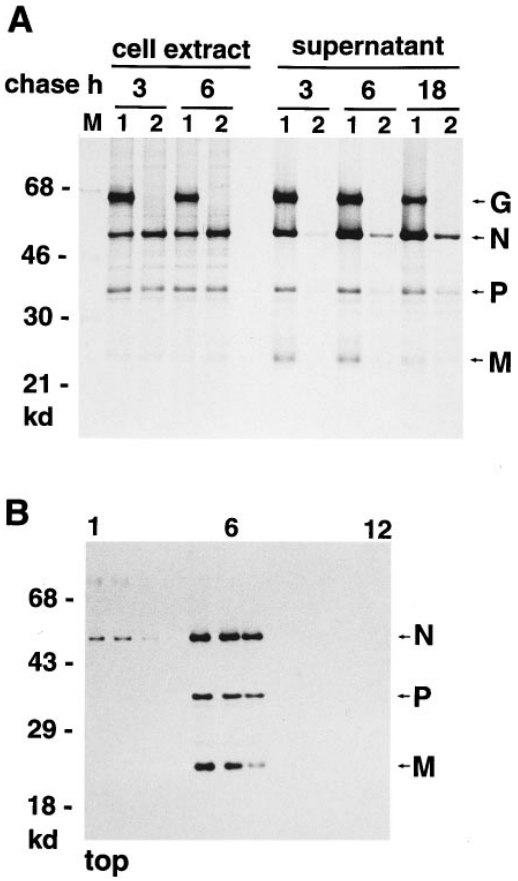

Figure 7. Formation of Spikeless Rhabdovirus Particles

(A) Cells infected at a moi of 1 with SAD L16 or with phenotypically complemented SAD ΔG were incubated for 16 hr and pulse labeled with 100 μCi of [^{35}S]methionine for 3 hr. After the indicated chase periods, virions were pelleted from the supernatant through a 20% sucrose cushion. Viral proteins from resuspended pellets and cell extracts were precipitated with an anti-RV rabbit serum (S71). Lanes 1, SAD L16; lanes 2, SAD ΔG. Labeled bands corresponding to N, P, and M proteins were excised from the dried gel, and radioactivity was determined by scintillation counting.

(B) Purification of spikeless SAD ΔG virus particles by velocity centrifugation in sucrose gradients. Supernatant from 6×10^6 cells (i.e., the 6-fold amount of material used for the experiments shown in Figure 5), infected with phenotypically complemented SAD ΔG, was processed as described for Figure 5.

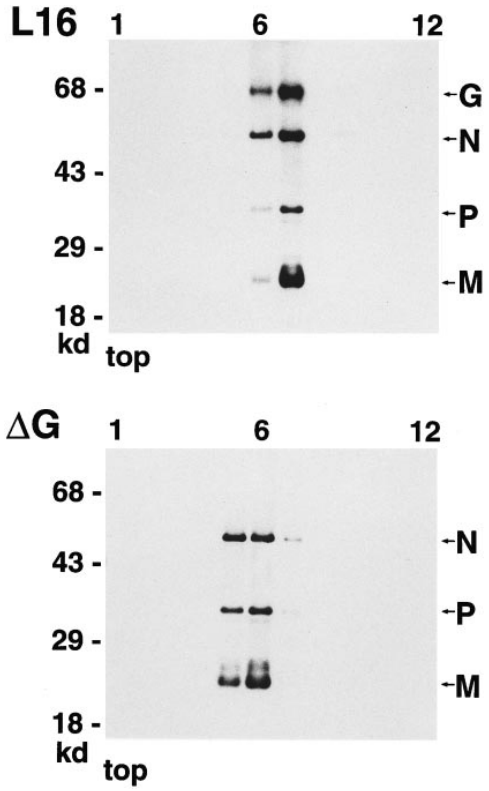

Figure 8. Determination of the Density of Spikeless RV Particles

SAD L16 or SAD ΔG virions were first purified by pelleting on a 60% sucrose cushion and sedimented to equilibrium in continuous 10%–70% sucrose gradients. Gradient fractions were analyzed by immunoblotting. The sucrose density was determined from the refractive index of each fraction (lane 6, 1.14 g/cm^3; lane 7, 1.16 g/cm^3).

had been found to be reduced by a factor of 5, 2.5, and 2, respectively (data not shown).

To characterize the structure of the material released from SAD ΔG-infected cells, we analyzed the supernatants by sucrose gradient centrifugation. After infection of cells, inactivation of input virus by anti-RV serum, and subsequent incubation for 2 days, supernatants were fractionated by velocity centrifugation and analyzed by Western blotting. As previously observed for SAD L16 and SAD ΔCD (Figure 5), the N, P, and M proteins were present in fractions 5, 6, and 7 (Figure 7B) and showed the same ratios as in standard virions, indicating that the material is released exclusively in the form of spikeless rhabdovirus-sized particles. However, to obtain a signal comparable to that observed with SAD ΔCD (see Figure 5), the 6-fold amount of supernatant had to be applied on the gradient. Compared with standard virus, this suggests that an approximately 30-fold lower number of particles were produced in the absence of the spike glycoprotein. As verified by isopycnic centrifugation in continuous 10%–70% sucrose gradients, SAD ΔG particles were of uniform density and contained a lipid bilayer envelope. Interestingly, compared with standard SAD L16 virus, a slightly lower density was observed for the spikeless particles. Whereas the majority of SAD L16 virus was found in the fraction with a density of 1.16 g/cm^3 (Figure 8, fraction 7; Sokol et al., 1968), the majority of SAD ΔG particles sedimented to a density of 1.14 g/cm^3 (Figure 8, fraction 6). After treatment with 0.05% Triton, RNP complexes of both SAD L16 and SAD ΔG sedimented to a sucrose density of 1.21 g/cm^3 (data not shown), demonstrating that the mutant virus differs from wild type only in its membrane protein composition. Direct evidence for the assembly and budding of typical rhabdovirions was further obtained by electron microscopy. Virions budding from the cell surface membrane possessed typical rhabdovirus shape but failed to be labeled by immunogold (Figures 6E and 6F).

Discussion

Rhabdoviruses have been widely used as model viruses to study individual functions of membrane proteins.

However, it has not been possible to determine whether a functional link exists between sorting and incorporation of spike glycoproteins on the one hand and the budding process on the other. This was due to the fact that their genomes have not been amenable to specific alteration. We have now succeeded in generating defined recombinant virus mutants that allowed dissection of the roles of RV G protein in the viral assembly process. In particular, this reverse genetics approach profited from the absolute absence of helper virus as well as the possibility to *trans*-complement a mutant lacking essential functions.

To determine whether an interaction of the RV spike protein with the internal M protein or the RNP is crucial for initiation of the budding process and generation of virions, we constructed the mutant virus genome of SAD ΔCD to encode a carboxy-terminally truncated spike protein. According to the proposed structure of the RV G protein (Anilionis et al., 1981), the mutant protein lacks not only the entire cytoplasmic tail of the protein but also two cysteine residues that are assigned to the transmembrane domain and that in some RV strains may function as palmitoylation acceptors (Gaudin et al., 1991). Thus, none of the ΔCD amino acids should pass the lipid bilayer and be exposed at the cytoplasmic face of the membrane. The finding of autonomously propagating infectious agents demonstrated not only that the tailless G protein was present in the envelope of virions but also that it retained the ability to mediate an infection. Furthermore, electron-microscopic examination and gradient centrifugation revealed that particles budding from the surface membrane of cells infected with SAD ΔCD were of typical rhabdovirus shape. These results demonstrate that the cytoplasmic portion of the single RV spike protein and its presumed interaction with internal virus proteins is required neither for the initiation of budding nor for the release of mature virions.

Although the lack of the cytoplasmic tail does not abrogate the formation of rhabdovirus particles, the recombinant SAD ΔCD exhibited obvious phenotypic differences from wild-type virus possessing a complete G protein. Since replication and gene expression of the mutant virus was not affected by the deletion of the carboxy-terminal part of the G gene and since similar cell surface expression was observed for both the truncated and the standard G protein, the reduced rate of spread and the lower final titers of SAD ΔCD have to be assigned to inherent functions of the truncated G protein. In other studies, it has been clearly demonstrated that the cytoplasmic domain of the VSV G protein contributes to the specificity of incorporation into the viral envelope (Whitt et al., 1989). Moreover, it possesses an independent signal capable of directing a foreign protein into VSV particles. A chimeric spike protein, in which the HIV-1 gp160 ectodomain and transmembrane anchor domain was fused to the cytoplasmic tail of VSV G protein, rescued the infectivity of the temperature-sensitive VSV mutant *tsO45* at nonpermissive temperature (Owens and Rose, 1993). Since the envelope of *tsO45* virions generated at nonpermissive temperature contains a full complement of truncated VSV G protein fragments encompassing the cytoplasmic and transmembrane domains (Metsikkö and Simons, 1986), this approach could not reveal whether the cytoplasmic tail of the chimeric protein contributed to the budding process.

The absence of any cytoplasmic domain sequences in SAD ΔCD was therefore predicted to affect at least the incorporation of spikes into the viral membrane. This was supported by the finding of a markedly lower overall content of G protein in gradient-purified SAD ΔCD virions. Furthermore, immunogold labeling experiments revealed that the budding particles individually differed in their G content, confirming that in the absence of the cytoplasmic tail the specificity of incorporation and the resulting host cell exclusion is considerably hampered. However, budding of virion particles into supernatants was only reduced by a factor of approximately 5, as estimated from the gradient experiments (Figure 5). With regard to the assumed random incorporation of tailless spike proteins, as well as the variable G content of virions, the 10-fold reduction of infectious titers of SAD ΔCD observed after infection of cells at a moi of 1 also appeared moderate.

The finding that an interaction of the G protein with an internal component of the virus does not represent a prerequisite for initiation of budding prompted us to investigate whether the spike protein is at all necessary for virion formation. Therefore, a virus mutant lacking the entire G gene was generated. As presumed, after cells had been infected by phenotypically complemented SAD ΔG, the infection was not able to spread to surrounding cells and could not be passaged to other cell cultures. However, enveloped particles of defined density, and with sedimentation properties as well as protein ratios identical to those of rhabdovirions, were present in the cell culture supernatants. As confirmed by electron microscopy, these particles resulted from typical budding from the cell surface membrane. Thus, viral RNPs that are surrounded by M protein are able to drive the budding process in the absence of G protein. Obviously, the envelope of the generated particles should be distinguished from that of wild-type virions by the absence of the tight surface structure made up by the viral glycoprotein. Since it is likely that host cell protein exclusion during the viral assembly process is at least incomplete in the absence of the spike protein, we assume that the spikeless envelope contains diverse cell surface proteins. This difference might explain, at least in part, the slightly lower density of SAD ΔG particles as compared with wild-type virions (Figure 8).

The finding that viral "cores," i.e., RNPs surrounded by M protein, possess an autonomous exocytotic capability suggests on first sight that rhabdoviruses use an exocytosis mechanism that is different from that of alphaviruses and rather similar to that of retroviruses. In alphaviruses, budding of cores depends absolutely on the presence of the transmembrane spike glycoprotein E2 (Suomalainen et al., 1992) and most certainly on a direct interaction of the core and the E2 cytoplasmic domain (Zhao et al., 1994). In contrast, part of the internal retrovirus Gag protein is sufficient to induce efficient formation of particles (Delchambre et al., 1989; Gheysen et al, 1989; Rhee et al., 1990). Both the AD2 region of Gag and the rhabdovirus M protein are membrane-associated proteins possessing hydrophilic stretches and, in form of oligomeric assemblies, might cause

evagination of membranes either by executing an active "push" force or by displacing resident membrane proteins that prevent spontaneous exocytosis (Hunter, 1994). More direct evidence that the M protein is involved in rhabdovirus budding has been obtained for VSV. After expression of VSV M protein in the absence of other viral proteins, it was exported from both insect and mammalian cells within liposomes (Li et al., 1993; Justice et al., 1995).

Interestingly, however, the presence of RV G protein on the cell surface, even in the form of a truncated protein lacking the cytoplasmic tail and not able to interact directly with other viral proteins, was found to facilitate virus budding. While for wild-type or SAD ΔCD virus gradients the supernatant of one cell culture dish was sufficient to demonstrate virus particles (Figure 5), the 6-fold amount was necessary to obtain a comparable picture for the spikeless particles (Figure 7B). Accordingly, the presence of the spike glycoprotein increases budding efficiency approximately 30-fold. This indicates that, in addition to M, the RV G protein possesses an autonomous exocytosis activity. This conclusion is strongly supported by a recent report in which it was shown that VSV G expressed from a SFV replicon RNA is able to mobilize the vector RNA (Rolls et al., 1994). Infectious structures containing VSV G protein and randomly incorporated SFV replicons were apparently generated by budding from the cell membrane. In the same system, infectious vesicles containing RV G protein were also found in the supernatants, but the titers of 10^2/ml were at least 100-fold below those obtained with the VSV G protein (Rolls et al., 1994). This difference was attributed to the slower transport of the RV G protein to the cell surface. However, our own experiments (unpublished data) indicate that the intrinsic force of the RV and VSV G proteins to induce exocytotic budding are different. The present study demonstrates that this activity resides in the external part of the proteins.

Accordingly, we favor a model in which the highly efficient budding of rhabdovirus particles is ensured by a concerted action of two proteins possessing individual and independent exocytotic activities, namely, the "push" (bending of the membrane from the inside) and "pull" (bending of the membrane from the outside) activity of the rhabdovirus M and G proteins, respectively. Under optimal conditions, as in the case of standard virus budding, both exocytosis activities are brought together as close as possible by means of specific protein sorting. Obviously, the cytoplasmic tail of the spike protein contributes considerably to sorting, presumably by direct interaction with internal virus proteins. By this direct sorting, virions are generated that possess the highest density of exocytotically active proteins, namely, RNPs tightly enclosed in M protein and enwrapped by a membrane with the maximium amount of G protein. Such viruses are predicted to bud more efficiently than particles with a lower content of spikes or no spikes at all. However, as indicated by the effective production of infectious SAD ΔCD virions, a second, indirect means of sorting may exist. Accordingly, also in the absence of the cytoplasmic domain, the pull activity of the truncated G protein may add to the push activity of M-coated RNPs and facilitate budding of viral particles from membrane areas containing tailless spike protein assemblies. Indirect sorting by push and pull activities of proteins provides an attractive explanation for the paradox of phenotypic mixing between unrelated viruses (reviewed by Zavada, 1982) and the possibility of generating certain virus pseudotypes. Significantly, retrovirus (rhabdovirus) pseudotypes are observed frequently (e.g., Moloney retrovirus pseudotypes containing the VSV G protein can be obtained at high titers) (Burns et al., 1993). Since it is unlikely that the VSV spikes may interact with retroviral capsid proteins (Rose and Gallione, 1981), an explanation for how they are recruited into the retroviral virions is lacking (Dong et al., 1992). According to the conclusions drawn from this study, the strong pull activity of VSV G may add to the proven push activity of the retrovirus matrix protein and, thus, budding of viral particles from membrane areas containing many VSV spikes is considerably favored.

The opportunity to generate recombinant virion particles that are completely devoid of their own envelope proteins holds great promise with regard to several biomedical applications of rhabdovirus vectors. The generation of genetically engineered viruses or pseudotype viruses carrying foreign envelope proteins and possessing a tropism directed by the foreign envelope protein may prove to be simpler than expected. While approaches in retrovirus systems are now mostly aimed at extending the restricted host range of the viruses in order to develop vectors for gene therapy, the broad host ranges of rhabdoviruses and other negative-strand RNA viruses might be restricted in the future by the incorporation of defined surface glycoproteins. Approaches using such RNA viruses for specific cell targeting and transient gene therapy may have advantages over those involving viruses with a DNA phase.

Experimental Procedures

Construction of cDNA Clones

The full-length cDNA clone pSAD L16 (Schnell et al., 1994) that possesses the authentic sequence of the RV strain SAD B19 (Conzelmann et al., 1990) served as a basis for the assembly of pSAD ΔCD. Deletion of the sequence encoding the cytoplasmic domain of RV G protein and simultaneous introduction of a transcriptional stop codon was achieved through digestion of pT7T-G (Conzelmann and Schnell, 1994) with AflIII (position 4752 of the SAD B19 sequence), fill-in with Klenow enzyme, and religation to the EcoRV-cut multiple cloning site (Figure 1). A 0.3 kb PpuMI–SmaI fragment (SAD B19 position 4469 multiple cloning site) from the resulting plasmid containing the newly generated translation stop codon (underlined) that is composed of 2 RV and 1 vector-derived nucleotide (italics) and 17 additional nucleotides of the multiple cloning site (TGA *TCGAATT CCTGCAGCCC*) was introduced into pPsiX8 (Schnell et al., 1994) containing part of the SAD B19 sequence (3823–6668) that had been digested with BstXI (SAD B19 position 4995), filled in with Klenow, and then digested with PpuMI (pPsiX8ΔCD). The final pSAD ΔCD was obtained by replacement of the StuI fragment of pSAD L16 (SAD B19 position 4014–6364) with that of pPsiX8ΔCD. The manipulation resulted in a genome sequence in which the parental SAD B19 nucleotides 4753–4995 were replaced by 18 vector-derived sequences. To delete the entire G protein coding region from the RV genome, we used the full-length clone pSAD U2 (Schnell et al., 1994). This clone differs from pSAD L16 by the presence of a unique NheI site within the nontranslated 3′ region of the G gene (SAD B19 position 5339). By partial digestion of pSAD U2 with PflMI (SAD position 3176) and complete digestion with NheI, subsequent fill-in

by Klenow enzyme, and religation, a cDNA fragment comprising SAD B19 nucleotides 3177–5339 was removed (Figure 1A).

Rescue of Recombinant Viruses

Transfection experiments were carried out as described previously (Conzelmann and Schnell, 1994). Approximately 10^6 BSR cells were grown in 3.2 cm diameter culture dishes and infected with the recombinant vaccinia virus vTF7-3 expressing T7 RNA polymerase (provided by T. Fuerst and B. Moss; Fuerst et al., 1986). After 1 hr of adsorption, cells were transfected with a plasmid mixture containing 5 μg of pT7T-N, 2.5 μg of pT7T-P, 2.5 μg of pT7T-L, and 2 μg of pT7T-G and with 4 μg of pSAD ΔCD or pSAD ΔG, by using the Stratagene mammalian transfection kit ($CaPO_4$ protocol). Isolation of transfectant viruses and removal of vaccinia virus was carried out as described previously (Schnell et al., 1994). Cells were suspended in the culture supernatant 2 days after transfection and subjected to 3 cycles of freezing and thawing. Samples were clarified by centrifugation (10,000 × g in a microfuge) and used to inoculate fresh monolayers. For passage of SAD ΔG that required complementation with G protein, cells were incubated with the clarified inoculum for 2 hr, infected with vTF7-3, and transfected with 2 μg of pT7T-G as described above. Vaccinia virus–free RV stocks were prepared after four to five serial passages by filtration of supernatants through a 0.1-μm filter (Millipore Products).

Immunofluorescence Microscopy

For the detection of replicating RV, infected cells were fixed with 80% acetone and stained with a conjugate containing a mixture of MAbs directed to RV N protein (Centocor). Cell surface expression was monitored by incubating infected live cells with a 1:100 dilution of anti-RV G protein MAb E543 (Schneider and Meyer, 1981) and staining with a fluorescein isothiocyanate (FITC)-conjugated goat anti-mouse IgG antibody (Sigma; 1:200). Cells were fixed in 4% paraformaldehyde for 5 min and examined by fluorescence microscopy.

Analysis of RNA and RT–PCR

Total RNA isolated from infected cells was electrophoresed on a denaturing gel and analyzed by Northern blot hybridizations, as described previously (Conzelmann et al., 1991). RV N or G gene DNA fragments were labeled with ^{32}P by nick translation (nick translation kit, Amersham). RT–PCR was performed on 1 μg of total RNA from infected cells. Reverse transcription by AMV reverse transcriptase was primed by an RV G gene–specific oligonucleotide, *G6P* (5′-GACTTGGGTCTCCCGAACTGGGG-3′, SAD B19 nucleotides 4664–4686) or an M-gene specific primer, *M3P* (5′-AAGTGTGT AGCCCGAATG-3′,SAD B19 nucleotides 2674–2691). DNA amplification was done using one of the above primers and an L gene–specific primer, *L4M* (5′-CAAAGGAGAGTTGAGATTGTAGTC-3′, SAD B19 nucleotides 5516–5539), as described previously (Schnell et al., 1994). The PCR products resulting from 30 cycles (denaturation for 30 s at 94°C; annealing for 60 s at 45°C; elongation for 120 s at 72°C) were analyzed on 1% agarose gels and used directly for sequencing.

Metabolic Labeling, Immunoprecipitation, and Enzymatic Modification of Proteins

Approximately 10^6 BSR cells were infected with recombinant RVs at a moi of 1. After 16 hr of infection, cells were labeled with 50 μCi of [^{35}S]methionine (>1,000 Ci/mmol; Amersham) for 3 hr. Labeled antigen was extracted as described previously (Mebatsion et al., 1995), incubated with specific antisera, and precipitates were formed with cross-linked Staphylococcus aureus (Kessler, 1981). For pulse–chase experiments, infected cells were labeled for 10 min as above and incubated with chase medium for increasing times. In deglycosylation experiments, immunoprecipitated proteins were split into two equal aliquots and incubated in the absence or presence of Endoglycosidase H (New England Biolabs, Incorporated) or peptide N-glycosidase F (New England Biolabs, Incorporated), respectively, for 16 hr according to the instructions of the manufacturer. Tunicamycin treatment was done by adding 2 μg/ml of tunicamycin to the infected cells starting at 90 min prior to labeling. For surface immunoprecipitation, cells were infected at a moi of 1 and labeled with 100 μCi of [^{35}S]methionine (>1000 Ci/mmol) for 3 hrs at 16 hpi. Live cells were directly incubated with a 1:20 dilution of anti-G MAb 120-6 (Wunner et al., 1985) for 45 min at 4°C and lysed after removal of excess antibody. In control experiments, unlabeled infected cells were incubated with the anti-G MAb and subsequently lysed in the presence of extracts from infected labeled cells. Antigen extraction and immunoprecipitation were performed as described above. Immunoprecipitated proteins were analyzed by SDS–polyacrylamide gel electrophoresis and processed by fluorography with En^{3}Hance (New England Nuclear). To determine the amount of radioactivity in viral proteins from cells or virions, we excised labeled bands from the gels, digested them with Solvable (Packard), and mixed them with 2 ml of Ready Protein+ liquid scintillation fluid (Beckman Instruments, Incorporated). Radioactivity was measured on a Betaszint BF 8000 liquid scintillation counter.

Sucrose Gradient Centrifugation

Approximately 10^6 cells were infected with SAD L16 or SAD ΔCD and 6×10^6 cells with SAD ΔG at a moi of 1. For velocity centrifugation, the culture supernatants were collected 2 days postinfection and layered on 10%–50% sucrose gradients prepared in TEN buffer (10 mM Tris [pH 7.4], 50 mM NaCl, 1 mM EDTA). The gradients were centrifuged at 27,000 rpm in an SW41 rotor for 1 hr. Prior to isopycnic centrifugation particles from the supernatants of 2×10^5 (SAD L16), 1×10^6 (SAD ΔCD), and 6×10^6 cells (SAD ΔG) were purified by pelleting onto a 60% sucrose cushion and layered on 10%–70% continuous sucrose gradients directly or after treatment with 0.05% Triton X-100 for 20 min at room temperature. Samples were centrifuged in an SW41 rotor at 35,000 rpm (210,000 × g) for 18 hr. Equal amounts of 12 fractions were collected, and aliquots were used to determine the refractive index and the titer of infectious SAD L16 and SAD ΔCD particles. Particles were pelleted by centrifugation at 45,000 rpm in a TLA 45 rotor for 1 hr and resuspended in lysis buffer (2% SDS, 62.5 mM Tris, 10% glycerol, 6 M urea, 0.01% bromphenol red, 0.01% phenol red, and 5% mercaptoethanol).

Immunoblotting

Virus proteins from gradient fractions were resolved by SDS–polyacrylamide gel electrophoresis and transferred to nitrocellulose membrane (Schleicher and Schuell) in a semidry transfer apparatus (Hoefer Scientific Instruments). After incubation with blocking solution (2.5% dry milk, 0.05% Tween 20 in PBS) at room temperature for 1 hr, membranes were incubated overnight with a mixture of rabbit sera raised against purified RV G protein (S72; 1:20,000), purified RV ribonucleoprotein (S50; 1:20,000) and an anti-peptide serum specific for RV M protein (M1-B4; 1:10,000) in PBST (0.05% Tween 20 in PBS). The blot was then incubated for 2 hr with peroxidase-conjugated goat anti-rabbit IgG (Dianova) diluted 1:10,000 in PBST, and proteins were visualized by using the ECL Western blot detection kit (Amersham; 1 min incubation) and exposition to X-ray films (Biomax MR, Kodak).

Immunoelectron Microscopy

About 10^6 BSR cells were infected with recombinant viruses at a moi of 1. At 24 hpi, cells were fixed with 1% glutaraldehyde, and nonspecific binding sites were saturated with 1% bovine albumin. Cells were incubated overnight with a MAb (E543, Schneider and Meyer, 1981) directed against RV G protein at 4°C, and immunostaining was performed by incubating the samples with goat anti-mouse IgG antibody (Biocell, Cardiff) coupled to 10 nm gold particles. Cells were then treated with 2.5% glutaraldehyde and subsequently postfixed in 1% osmium tetraoxide and stained with 1% uranyl acetate (pH 4.3). Preparations were dehydrated in graded ethanols and embedded in Epon 812 (Serva). Following heat polymerization, the resin-embedded cell layers were mechanically removed from the culture dishes. Ultrathin sections were transferred to formvar- and carbon-coated glow-discharged copper–rhodium grids and stained with lead citrate and uranyl acetate. Noninfected BSR cells or infected cells incubated only with the secondary antibody were treated similarly to serve as controls. Specimens were examined in a ZEISS EM902 electron microscope. Micrographs were taken at an instrumental magnification of 30,000× on Kodak SO-163 film.

Acknowledgments

We thank Karin Pietschmann, Veronika Schlatt, and Uli Wulle for their expert technical assistance and Gregor Meyers, Tillman Rümenapf, and Jim Cox for valuable suggestions on the manuscript. This work was supported by grant BEO21/0310118A from the Bundesministerium für Bildung, Wissenschaft, Forschung und Technologie.

Received August 1, 1995; revised January 24, 1996.

References

Anilionis, A., Wunner, W.H., and Curtis, P.J. (1981). Structure of the glycoprotein gene of rabies virus. Nature *294*, 275–278.

Bruss, V., and Ganem, D. (1991). The role of envelope proteins in hepatitis B virus assembly. Proc. Natl. Acad. Sci. USA *88*, 1059–1063.

Burns, J.C., Friedmann, T., Driever, W., Burrascano, M., and Yee, J.-K. (1993). Vesicular stomatitis virus G glycoprotein pseudotyped retroviral vectors: concentration to very high titer and efficient gene transfer into mammalian and nonmammalian cells. Proc. Natl. Acad. Sci. USA *90*, 8033–8037.

Chong, L.D., and Rose, J.K. (1993). Membrane association of functional vesicular stomatitis virus matrix protein *in vivo.* J. Virol. *67*, 407–414.

Chong, L.D., and Rose, J.K. (1994). Interactions of normal and mutant vesicular stomatitis virus matrix proteins with the plasma membrane and nucleocapsids. J. Virol. *68*, 441–447.

Conzelmann, K.-K., and Schnell, M. (1994). Rescue of synthetic rabies virus genome analogs by plasmid encoded proteins. J. Virol. *68*, 713–719.

Conzelmann, K.-K., Cox, J.H., Schneider, L.G., and Thiel, H.-J. (1990). Molecular cloning and complete nucleotide sequence of the attenuated rabies virus SAD B19. Virology *175*, 485–499.

Conzelmann, K.-K., Cox, J.H., and Thiel, H.-J. (1991). An L (polymerase) deficient rabies virus defective interfering particle RNA is replicated and transcribed by heterologous helper virus L proteins. Virology *184*, 655–663.

Delchambre, M., Gheysen, D., Thines, D., Thiriart, C., Jacobs, E., Verdin, E., Horth, M., Burny, A., and Bex, F. (1989). The GAG precursor of simian immunodeficiency virus assembles into virus-like particles. EMBO J. *8*, 2653–2660.

Dong, J., Roth, M.G., and Hunter, E. (1992). A chimeric avian retrovirus containing the influenza virus hemagglutinin gene has an expanded host range. J. Virol. *66*, 7374–7382.

Fuerst, T.R., Niles, E.G., Studier, F.W., and Moss, B. (1986). Eukaryotic transient expression system based on recombinant vaccinia virus that synthesizes bacteriophage T7 RNA polymerase. Proc. Natl. Acad. Sci. USA *83*, 8122–8126.

Gaudin, Y., Tuffereau, C., Benmansour, A., and Flamand, A. (1991). Fatty acylation of rabies virus proteins. Virology *184*, 441–444.

Gheysen, D., Jacobs, E., deForesta, F., Thiriart, C., Francotte, M., Thines, D., and DeWilde, M. (1989). Assembly and release of HIV-1 precursor Pr55*gag* virus-like particles from recombinant baculovirus–infected insect cells. Cell *59*, 103–112.

Hunter, E. (1994). Macromolecular interactions in the assembly of HIV and other retroviruses. Semin. Virol. *5*, 71–83.

Jin, H., Leser, G.P., and Lamb, R.A. (1994). The influenza virus hemagglutinin cytoplasmic tail is not essential for virus assembly or infectivity. EMBO J. *13*, 5504–5515.

Justice, P.A., Sun, W., Li, Y., Ye, Z., Grigera, P.R., and Wagner, R.R. (1995). Membrane vesiculation function and exocytosis of wild-type and mutant matrix proteins of vesicular stomatitis virus. J. Virol. *69*, 3156–3160.

Kessler, S.W. (1981). Use of protein A–bearing staphylococci for the immunoprecipitation and isolation of antigens from cells. Meth. Enzymol. *73*, 442–459.

Lawson, N.D., Stillman, E.A., Whitt, M.A., and Rose, J.K. (1995). Recombinant vesicular stomatitis viruses from DNA. Proc. Natl. Acad. Sci. USA *92*, 4477–4481.

Li, Y., Luo, L., Schubert, M., Wagner, R.R., and Kang, C.-Y. (1993). Viral lyposomes released from insect cells infected with recombinant baculovirus expressing the M protein of vesicular stomatitis virus. J. Virol. *67*, 4415–4420.

Mebatsion, T., Schnell, M.J., and Conzelmann, K.-K. (1995). Mokola virus glycoprotein and chimeric proteins can replace rabies virus glycoprotein in the rescue of infectious defective rabies virus particles. J. Virol. *69*, 1444–1451.

Metsikkö, K., and Simons, K. (1986). The budding mechanism of spikeless vesicular stomatitis virus particles. EMBO J. *5*, 1913–1920.

Owens, R.J., and Rose, J.K. (1993). Cytoplasmic domain requirement for incorporation of a foreign envelope protein into vesicular stomatitis virus. J. Virol. *67*, 360–365.

Rhee, S.S., Hui, H., and Hunter, E. (1990). Preassembled capsids of type D retroviruses contain a signal sufficient for targeting specifically to the plasma membrane. J. Virol. *64*, 3844–3852.

Rolls, M.M., Webster, P., Balba, N.H., and Rose, J.K. (1994). Novel infectious particles generated by expression of the vesicular stomatitis virus glycoprotein from a self- replicating RNA. Cell *79*, 497–506.

Rose, J.K., and Bergmann, J.E. (1983). Altered cytoplasmic domains affect intracellular transport of the vesicular stomatitis virus glycoprotein. Cell *34*, 513–524.

Rose, J.K., and Gallione, C.J. (1981). Nucleotide sequence of the mRNAs encoding the vesicular stomatitis virus G and M proteins determined from cDNA clones containing the complete coding regions. J. Virol. *39*, 519–528.

Schneider, L., and Meyer, S. (1981). Antigenic determinants of rabies virus as demonstrated by monoclonal antibody. In The Replication of Negative Strand Viruses, D.H.L. Bishop and R. W. Compans, eds. (Amsterdam: Elsevier), pp. 947–953.

Schnell, M.J., Mebatsion, T., and Conzelmann, K.-K. (1994). Infectious rabies viruses from cloned cDNA. EMBO J. *13*, 4195–4203.

Simons, K., and Garoff, H. (1980). The budding mechanisms of enveloped animal viruses. J. Gen. Virol. *50*, 1–21.

Sokol, F., Kuwert, E., Wiktor, T.J., Hummeler, K., and Koprowski, H. (1968). Purification of rabies virus grown in tissue culture. J. Virol. *2*, 836–849.

Suomalainen, M., Liljeström, P., and Garoff, H. (1992). Spike protein–nucleocapsid interactions drive the budding of alphaviruses. J. Virol. *66*, 4737–4747.

Whelan, S.P.J., Ball, L.A., Barr, J.N., and Wertz, G.T.W. (1995). Efficient recovery of infectious vesicular stomatitis virus entirely from cDNA clones. Proc. Natl. Acad. Sci. USA *92*, 8388–8392.

Whitt, M.A., Chong, L., and Rose, J.K. (1989). Glycoprotein cytoplasmic domain sequences required for rescue of a vesicular stomatitis virus glycoprotein mutant. J. Virol. *63*, 3569-3578.

Whitt, M.A., Buonocore, L., Prehaud, C., and Rose, J.K. (1991). Membrane fusion activity, oligomerization and assembly of the rabies virus glycoprotein. Virology *185*, 681–688.

Wunner, W.H.B., Dietzschold, B., Macfarlan, R.I., Smith, E., Golub, E., and Wiktor, T.J. (1985). Localization of immunogenic domains on the rabies virus glycoprotein. Ann. Inst. Pasteur (Paris) *136E*, 353–362.

Zavada, J. (1982). The pseudotypic paradox. J. Gen. Virol. *63*, 15–24.

Zhao, H., Lindqvist, B., Garoff, H., von Bonsdorff, C.-H., and Liljeström, P. (1994). A tyrosine-based motif in the cytoplasmic domain of the alphavirus envelope protein is essential for budding. EMBO J. *13*, 4204–4211.